

# **Molecular Origin of Internal Friction in Intrinsically Disordered Proteins**

**Priyasha Deshpande**

**A dissertation submitted for the partial fulfillment of BS-MS dual degree in Science**



**Department of Chemical Sciences**

**Indian Institute of Science Education and Research (IISER) Mohali**

**April 2019**

# **Certificate of Examination**

This is to certify that the dissertation titled “Molecular Origin of Internal Friction in Intrinsically Disordered Proteins” submitted by Ms. Priyasha Deshpande (MS14185) for the partial fulfillment of BS-MS dual degree programme of the Institute, has been examined by the thesis committee duly appointed by the Institute. The committee finds the work done by the candidate satisfactory and recommends the report be accepted.

Dr. Sabyasachi Rakshit

Dr. Angshuman Roychoudhury

Dr. Samrat Mukhopadhyay

(Supervisor)

# Declaration

The work presented in this dissertation has been carried out by me under the supervision of Dr. Samrat Mukhopadhyay at the Department of Chemical Sciences, Indian Institute of Science Education and Research (IISER) Mohali.

This work has not been submitted in part or full for a degree, a diploma, or a fellowship to any other university or institute.

Whenever contributions of others are involved, every effort is made to indicate this clearly, with due acknowledgment of collaborative research and discussions. This thesis is a bona fide record of original work done by me and all sources listed within have been detailed in the bibliography.

Date:

Priyasha Deshpande

In my capacity as a supervisor of the candidate's thesis work, I certify that the above statements by the candidate are true to the best of my knowledge.

Dr. Samrat Mukhopadhyay

(Supervisor)

## **Acknowledgements**

This dissertation is a result of collective efforts, contribution and support of a large number of people and I would like to take this opportunity to thank each and every one of them.

I would like to convey my deepest gratitude to Dr. Samrat Muhopadhyay for his constant support and motivation which gave me the confidence to pursue my scientific dreams. His passion for science and the ability to excite people about science is truly admirable. This journey would have been simply impossible without his guidance and enthusiastic approach. Over the years the lab has managed to maintain a thrilling scientific environment which inspired me throughout this year. Each and every member of the SM lab truly loves the science he/she does and there cannot be a greater inspiration than this to any undergraduate student.

I express my most sincere gratitude to Debapriya without whom this research would have been impossible. She has been an amazing teacher and understanding some of the toughest concepts related to internal friction would have been impossible without her. From protein purification to time-resolved anisotropy, she helped me understand each and every single thing in great detail.

I am thankful to all the former and present members of the SM lab for their constant support. Working in lab was always fun because of them. I owe my scientific and academic development to all these wonderful people. I thoroughly enjoyed working with all of them including Anupa, Swapnil, Priyanka Dogra, Priyanka Madhu, Aishwarya, Debapriya, Sayanta, Anamika, Sandeep and Anusha. I owe very special thanks to Ashish and Lisha for being super fun and cheerful throughout my tenure. I owe a special thanks to Achuthan with whom all the lab members had a lot of fun during the summer break.

I am thankful to Dr. S. Rakshit and Dr. A. Roychoudhuri for their comments, inputs and suggestions on my work. I am thankful to Prof. Vinod Subramaniam (University of Twente, The Netherlands) for providing us the human  $\alpha$ -synuclein plasmid. I am thankful to Prof. N. Periasamy (Retd. TIFR, Mumbai)

I am grateful to the Department of Science and Technology, Government of India for their financial support through the DST-INSPIRE fellowship program. I am thankful to IISER Mohali for providing a vibrant scientific environment and state-of-the-art facilities without which this research would not have been possible.

I consider myself extremely lucky to have found an amazing bunch of friends in life. I am grateful to have all these warm, loving and compassionate people in my life. My stay at IISER would have been impossible without Adarsh, Varun, Shriya, Siddhi, Awani, Vishnu, Shiny, Somak, Swadheen and, my coffee mates Sachin and Swetha. They managed to lift my spirits during the most difficult times.

Last, but not the least I would like to thank the most important people of my life, my parents and my brother Prathamesh for being extremely supportive and loving throughout my life. My parents are my biggest inspiration in life. I strive to be a little more like them each day. My mom is the single most important reason for my passion towards chemistry and biochemistry. I would take this opportunity to convey my deepest gratitude to my grandparents. I owe a very special thanks to my uncle, with whom I have had some of the most mind-blowing scientific and philosophical discussions and I hope to have many more in the future. I would like to thank my cousin Devesh for being extremely supportive and motivating me throughout this journey.

# List of Figures

**Figure 1:** (a) Diffusional barrier crossing problem for a one dimensional reaction coordinate in the context of protein folding. (b) Mathematical representation of Kramers' reaction rate theory where  $k$  is the rate of barrier crossing and constant  $A$  depends upon the curvatures of free energy function ( $\omega_a$  and  $\omega_b$ ). (c) Linear fit between rotational correlation time and solvent viscosity yields internal friction as an intercept on the Y-axis.

**Figure 2:** Schematic representation of a polypeptide backbone showing the dihedral angles  $\Phi$  and  $\Psi$ .

**Figure 3.** The sequence and different regions of human  $\alpha$ -synuclein protein. The underlined residue was mutated to cysteine. The mutant position is highlighted in black.

**Figure 4.** CD spectra of IAEDANS-labeled A18C  $\alpha$ -synuclein in different concentrations of sucrose.

**Figure 5.** Steady increase observed in the steady-state anisotropy with increase in sucrose content.

**Figure 6:** (a) Steady increase in IAEDANS anisotropy observed for IAEDANS-labeled  $\alpha$ -synuclein. (b) Schematic representation of IAEDANS-labeled human  $\alpha$ -synuclein protein.

**Figure 7:** (a) Picosecond time-resolved anisotropy decays of fluorescein [ $r(t)$ ] in different solvent. (b) Linear fit between rotational correlation time ( $\phi$ ) of fluorescein and the solvent viscosity (in centipoise)

**Figure 8:** Different modes of fluorescence depolarization arising due to different dynamical events

**Figure 9:** Different anisotropy decay profiles obtained in case of globular/collapsed proteins vs. IDPs. The segmental mobility arises due to the backbone torsional relaxation in the  $\Phi$ - $\Psi$  dihedral space.

**Figure 10:** (a) Picosecond time-resolved anisotropy decays of IAEDANS-labeled  $\alpha$ -synuclein [ $r(t)$ ] in different solvent viscosities. (b) Linear fit between the slow rotational correlation time components and dynamic viscosity of the solvent.

**Figure 11:** Scatter plot showing the fast rotational correlation time component scaling up with the rotational correlation time of fluorescein.

**Figure 12:** Normalized plot reveals that the rotational correlation time of fluorescein scales linearly with solvent viscosity and does not give rise to an intercept on the Y-axis, unlike the slow rotational correlation time component of IAEDANS-labeled protein.

# List of Tables

**Table 1:** Dynamic viscosities of different sucrose solutions at 20°C.

**Table 2:** Rotational correlation time of fluorescein in different concentrations of sucrose.

**Table 3:** Rotational correlation time components and their corresponding amplitudes for IAEDANS-labeled A18C  $\alpha$ -synuclein.



# Contents

<b>List of figures.....</b>	<b>i</b>
<b>List of Tables.....</b>	<b>iii</b>
<b>Abstract.....</b>	<b>vi</b>
<b>1. Introduction.....</b>	<b>1</b>
<b>2. Experimental Methods.....</b>	<b>4</b>
2.1 Materials.....	4
2.2 Protein expression and purification.....	4
2.3 Preparation of protein samples.....	5
2.4 Preparation of protein samples for steady-state and time-resolved fluorescence anisotropy measurements.....	7
2.5 Preparation of fluorescein samples for steady-state and time-resolved fluorescence anisotropy measurements.....	7
2.6 Circular Dichroism (CD) experiments.....	7
2.7 Steady-state fluorescence measurements.....	8
2.8 Time-resolved fluorescence measurements.....	8
<b>3. Results and Discussion</b>	
3.1 Circular Dichroism (CD) measurements.....	10
3.2 Steady-state fluorescence anisotropy measurements.....	11
3.3 Time-resolved fluorescence anisotropy measurements.....	13
<b>4. Conclusion and future outlook.....</b>	<b>20</b>
<b>5. Bibliography.....</b>	<b>21</b>

# Molecular Origin of Internal Friction in Intrinsically Disordered Proteins

Priyasha Deshpande

Department of Chemical Sciences

Indian Institute of Science Education and Research, Mohali

MS Thesis Supervisor: Dr. Samrat Mukhopadhyay

## Abstract

The work presented in this dissertation involves the study of dynamical aspects of an intrinsically disordered protein namely human  $\alpha$ -synuclein, which is a highly conserved pre-synaptic protein, and its aggregation is observed in the devastating Parkinson's Disease (PD) and other synucleinopathies.<sup>1</sup> Conformational dynamics of polypeptide chains is a diffusion-controlled process in the dense aqueous environment. Kramers' theory (Figure 1) provides a theoretical framework to explain such diffusion-controlled processes and states that the rate of protein folding or conformational relaxation is inversely proportional to solvent viscosity and directly proportional to "attempt frequency" of free energy barrier crossing<sup>2,7</sup>. Dynamical fluctuations giving rise to conformational changes in proteins are affected due to thermal changes and viscous drags experienced by proteins.<sup>3</sup> As opposed to simple polymeric systems or small molecules wherein the dynamics largely depends upon the solvent viscosity, proteins might show presence of certain internal energy dissipation mechanisms which will ultimately affect the conformational relaxation of polypeptides chains. This internal energy dissipation mechanism which offers inherent resistance to polypeptide chain towards changing its configuration is termed as internal friction.<sup>4</sup> Internal friction has been known to have an effect on the rate of conformational changes in proteins.<sup>5</sup> however, the molecular origin of this phenomenon remains elusive. The presence of internal friction can be attributed to several factors such as interchain collisions, dihedral angle rotations<sup>27</sup>, hydrogen bonding etc.<sup>6,25</sup> The aim of this study was to understand whether dihedral rotations of the polypeptide backbone contribute to the internal friction in case of a model IDP, namely  $\alpha$ -synuclein. In order to unravel the dihedral rotational dynamics, we took advantage of the powerful time-resolved fluorescence anisotropy measurements. The relationship between rotational dynamics and solvent viscosity is given by the Stokes-Einstein-Debye model.

The model relates the rotational correlation time of a particle to the bulk viscosity of the surrounding medium.<sup>8</sup> One of the most common and model independent ways to characterize internal friction is by plotting the rotational correlation time ( $\phi$ ) as a function of solvent viscosity.<sup>10</sup> Internal friction component is then obtained as an intercept on the Y-axis. In our experimental results we observed that the slow rotational correlation time component ( $\phi_{\text{slow}}$ ) of fluorophore-tagged protein does scale linearly with the solvent viscosity but an intercept is obtained on the Y-axis if the plot is extrapolated to zero viscosity. The slow rotational correlation time component ( $\phi_{\text{slow}}$ ) is known to correspond to the dihedral rotational relaxation time scale of the protein backbone in case of expanded IDPs.<sup>11</sup> Therefore even at zero viscosity, the protein seems to offer resistance towards changing its conformation. We suspect that this internal resistance offered by the protein arises due to the  $\Phi$ - $\Psi$  dihedral rotations of the polypeptide backbone over the Ramachandran dihedral space ultimately contributing to internal friction.

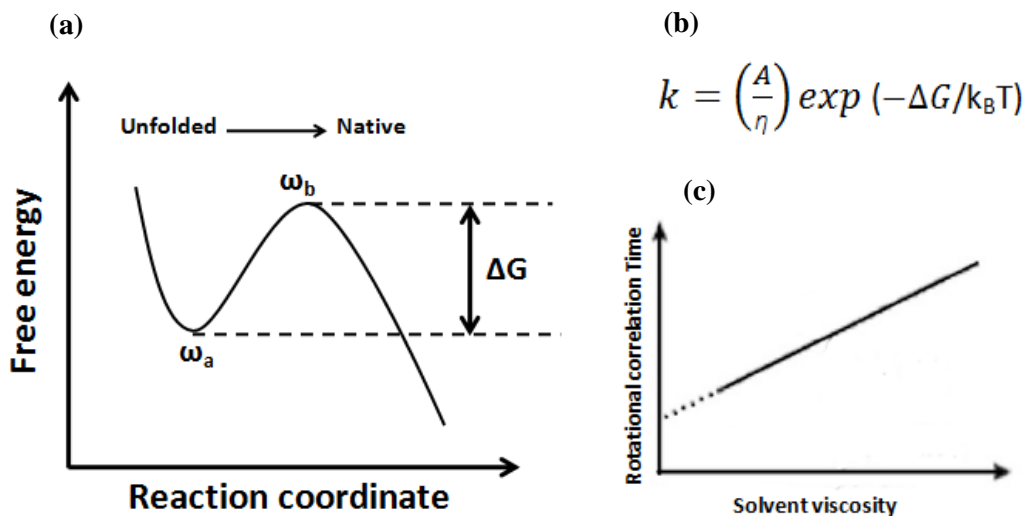


**Figure 1:** (a) Diffusional barrier crossing problem for a one dimensional reaction coordinate<sup>10</sup> in the context of protein folding. (b) Mathematical representation of Kramers' reaction rate theory where  $k$  is the rate of barrier crossing and constant  $A$  depends upon the curvatures of free energy function ( $\omega_a$  and  $\omega_b$ ). (c) Linear fit between rotational correlation time and solvent viscosity yields internal friction as an intercept on the Y-axis.

## 1. Introduction

The textbook sequence-structure-function paradigm states that correct folding of a polypeptide chain makes it a biologically functional entity and this folded conformation is indeed determined by the primary sequence of the protein.<sup>12</sup> However, a large fraction of the proteins from the entire proteome are known to lack a fixed 3-dimensional structure.<sup>13</sup> These proteins are known as Intrinsically Disordered Proteins (IDPs). IDPs show distinct compositional bias since they are enriched in charged and polar amino acid residues<sup>29</sup> such as lysine (K), glutamate (G) etc. and are depleted in hydrophobic and non-polar residues such as tryptophan (W), tyrosine (Y) etc. The lack of conformational rigidity governs IDPs the ability to bind to multiple cellular partners and perform different physiological functions.  $\alpha$ -synuclein is a small, 140 residue long, IDP primarily found in the presynaptic terminals of neurons and in other parts of the central nervous system (CNS). The sequence is divided into three domains (Figure 3)- N-terminal (1-60 amino acid residues, net positive charge) which has a net positive charge, NAC domain (Non-amyloid  $\beta$  component, 61-95 amino acid residues) which is known to form the core of the amyloid fibril<sup>14</sup> and C-terminal (96-140 amino acid residues, net negative charge) which is known to bind to calcium and other positively charged ions.<sup>15</sup> IDPs are known to adopt different conformations depending upon their binding partners therefore studying the conformational dynamics of IDPs can prove to be crucial in terms of elucidating the mechanism of their functionality.

Conformational dynamics of proteins is primarily dictated by the thermal fluctuations and the viscous force experienced by the protein chains. The net frictional force experienced by a polypeptide chain can be separated into two components. The first component known as the “wet” friction arises due to the solvent viscosity while the second component, known as the internal friction or the “dry” friction arises as a result of intra or inter chain interactions of the protein.<sup>4</sup> Presence of internal friction is known to have an effect on the conformational changes in proteins as it slows the protein dynamics down. The phenomenon of energy dissipation into internal coordinates of the polypeptide chain during conformational changes that ultimately do not contribute to overall protein dynamics is termed as internal friction.<sup>4</sup> Presence of internal friction in the protein chains finally results in increased “roughness” of the free energy landscape of proteins.<sup>3</sup> Internal friction may arise due to several factors such

as dihedral rotations in the polypeptide backbone, intra or inter chain interactions, intrachain collisions.<sup>6</sup> These factors ultimately slow down the conformational dynamics in proteins. We were interested in deciphering the molecular origin of internal friction in case of intrinsically disordered proteins. We chose human  $\alpha$ -synuclein, an expanded IDP, as our model system.

We posed the following question-

Does dihedral isomerisation i.e. dihedral angle rotation in the polypeptide chain contribute to internal friction in case of IDPs?

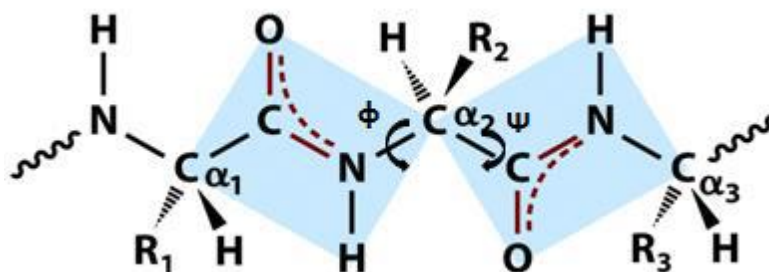


**Figure 2:** Schematic representation of a polypeptide backbone showing the dihedral angles  $\Phi$  and  $\Psi$ . In a polypeptide chain,  $\Phi$  is defined as the dihedral angle between C $\alpha$  and N while  $\Psi$  is the dihedral angle between C $\alpha$  and C.

In order to answer the posed question, we selected a model-independent method for characterizing internal friction. A linear fit between the rotational correlation time and the solvent viscosity yields internal friction as an intercept of the Y-axis.<sup>10</sup>

We used the powerful yet ultra-sensitive technique namely picosecond time-resolved fluorescence anisotropy to probe the dihedral rotational dynamics of the protein backbone. It has been previously established that the time-resolved fluorescence anisotropy decay profiles of a fluorophore-tagged IDP reveal two distinct rotational correlation time components. The first rotational correlation time ( $\phi_{\text{fast}}$ ) corresponds to the local diffusional motion of the fluorophore whereas the second rotational correlation time ( $\phi_{\text{slow}}$ ) arises due to the segmental mobility of the peptide backbone.<sup>11</sup> This segmental mobility is indeed a result of the dihedral

relaxation or torsional dynamics of the backbone (Figure 2). The Stokes-Einstein-Debye model relates the rotational correlation time to the solvent viscosity as follows-

$$\phi = \frac{\eta V}{k_B T} (fC)$$

Where  $\eta$  = Dynamic viscosity of solvent,  $\phi$  = Rotational correlation time,

$V$  = Molecular volume,  $f$  = Shape factor,  $C$  = Solute-solvent coupling parameter ( $C=1$  for our experiments)

$T$  = Temperature and,  $k_B$  = Boltzmann constant.

Since  $\alpha$ -synuclein is devoid of cysteine residues, single cysteine mutant namely A18C was previously created in the lab and we chose this construct for our studies. This cysteine residue was used for covalently tagging the protein with a fluorescent probe namely IAEDANS (1, 5-IAEDANS, 5-(((2-iodoacetyl) amino)ethyl)amino)naphthalene-1-sulfonic acid). Previous reports suggest that a model independent way of quantifying internal friction in case of proteins is by plotting the rotational correlation time ( $\phi$ ) as a function of solvent viscosity and extrapolating the plot to zero viscosity, where internal friction results as an intercept. The labeled protein was added to solutions of varied viscosities. Solutions of different viscosities were prepared by dissolving corresponding amount of sucrose in native buffer (20 mM tris, 50 mM NaCl, pH 7.4) and time-resolved anisotropy decays were collected which revealed the presence of two distinct rotational correlation time components as expected. As a proof of principle, we studied the rotational dynamics of a free probe, namely fluorescein, in varying concentrations of viscogen, i.e. sucrose. The depolarization kinetics revealed a single rotational correlation time for fluorescein which was seen to scale linearly with the solvent viscosity as per the Stokes-Einstein-Debye model. In case of protein the fast as well as slow rotational correlation time was seen to increase with an increase in solvent viscosity.  $\phi_{\text{fast}}$  was seen to follow the Stokes-Einstein-Debye model but  $\phi_{\text{slow}}$  did not scale up linearly with the solvent viscosity. Taking these results into account we confirmed our hypothesis to be true and we therefore suspect that the dihedral rotations could be major contributors to the internal friction and we suspect that this ultimately results in the roughness of the free energy landscape of the protein.

## 2. Experimental Methods

### 2.1 Materials:

IAEDANS (1, 5-IAEDANS, 5-(((2-iodoacetyl) amino)ethyl)amino)naphthalene-1-sulfonic acid) was purchased from Invitrogen. Free fluorescein dye was purchased from Fluka Analytical. Q (quaternary ammonium) sepharose fast flow resin for ion-exchange chromatography was purchased from GE Healthcare. LB (luria broth powder), tris, NaCl(sodium chloride) were procured from Hi-Media. HCl(Hydrochloric acid), ammonium sulfate, glacial acetic acid, ethanol were purchased from Merck. Ampicillin, IPTG (isopropyl  $\beta$ -D—thiogalactopyranoside) and chloramphenicol were purchased from Goldbio.com. EDTA (ethelenediaminetetraaceticacid), ammonium acetate and DTT (DL-dithiothreitol) were obtained from Sigma Aldrich while streptomycin sulfate was purchased from CDH and used as received.

### 2.2 Protein Expression and Purification:

$\alpha$ -synuclein mutant, namely A18C, was purified using previously reported protocol.<sup>16</sup> The pT7-7 plasmid (containing ampicillin resistance gene) with human  $\alpha$ -synuclein gene was provided by Prof. Vinod Subramaniam from the University of Twente, The Netherlands. The plasmid was previously transformed into BL21 (DE3) strain of *Escherichia coli*. To summarize briefly, roughly 1% of culture which was grown at 37°C overnight (containing 100  $\mu$ g/mL ampicillin and 35  $\mu$ g/ml chloramphenicol) was transferred into fresh media containing 100  $\mu$ g/mL ampicillin and incubated at 37° C until the O.D. reached 0.4-0.6. The culture was then induced with 800  $\mu$ g/mL IPTG and incubated at 30°C for 8 hours. The cell culture was then centrifuged at 4,000 rpm for 30 minutes at 4°C in order to obtain a cell pellet. The pellet was resuspended in lysis buffer (50 mM Tris, 150 mM NaCl, 10 mM EDTA, pH 8). The lysed cells were boiled at 100°C for 30 min and the lysate was then centrifuged at 11,500 rpm for 30 min at 4°C. The supernatant was collected and 136  $\mu$ L/mL 10% streptomycin and 228  $\mu$ L/mL glacial acetic acid was added to the supernatant in order precipitate DNA and RNA. The solution was then centrifuged at 11,500 rpm for 30 min at 4°C. The clear supernatant obtained after centrifugation was mixed with an equal volume of saturated ammonium sulfate and kept at 4°C for 2 hours in order to precipitate the protein of

interest. The precipitated protein was separated by centrifugation at 11,500 rpm at 4°C for 30 min. The obtained protein pellet was resuspended in ammonium acetate and 100% ethanol and followed by centrifugation at 4,000 rpm for 10 min. The pellet was again washed with 100% ethanol and dried at 37°C overnight. The pellet was dissolved in equilibrating buffer (10 mM Tris, 1 mM 2-mercaptoethanol, and pH 7.4) and purified on a Q Sepharose column. Protein was then eluted by adding 30 mL elution buffer (10 mM Tris, 500 mM NaCl, pH 7.4) and stored at -80°C for further use.

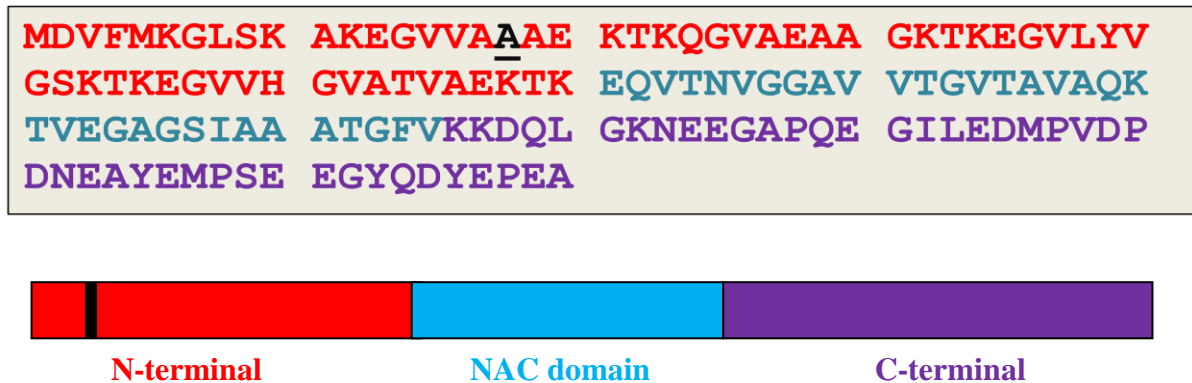


**Figure 3.** The sequence and different regions of human  $\alpha$ -synuclein protein. The underlined residue was mutated to cysteine. The mutant position is highlighted in black.

### 2.3 Preparation of protein samples-

#### Fluorescence labeling of A18C $\alpha$ -synuclein with IAEDANS:

Single cysteine mutant, A18C, of  $\alpha$ -synuclein was covalently labeled with a fluorescent probe namely IAEDANS (1, 5-IAEDANS, 5-(((2-iodoacetyl)amino)ethyl)amino)naphthalene-1-sulfonic acid) under reducing conditions. Initially,  $\alpha$ -synuclein was incubated in DTT (DL-dithiothreitol) for 30 min to ensure complete reduction of all disulfide bonds. From a freshly prepared stock (200mM) of IAEDANS (in DMSO) 8.75  $\mu$ L of dye was added and the mixture was incubated at room temperature for 1 hr 10 min. Again 8.75  $\mu$ L of dye was added and the mixture was incubated at room temperature for 1 hr 20 min. The labeling was carried out maintaining a final ratio of 1:3.5:20 for protein: DTT: dye. At the end of the reaction, labeled protein was eluted with native buffer (20 mM



Tris, 50 mM NaCl, pH 7.4) using a PD-10 column to remove the unreacted dye. Initial fractions of labeled protein were pooled together and the concentration was checked using UV-Vis spectroscopy molar extinction coefficient of  $6,100 \text{ M}^{-1} \text{ cm}^{-1}$ . The labeled protein was used for experiments.

**Preparation of sucrose solutions of different viscosities:** Sucrose solutions of different w/w percentage were prepared to achieve solutions of different viscosities.

**Table 1:** Dynamic viscosities of different sucrose solutions at 20°C are as follows.<sup>17</sup>

Sr. No.	w/w % sucrose	Dynamic Viscosity Centipoise (cP)
1	0	1.002
2	5	1.146
3	10	1.336
4	12	1.429
5	14	1.534
6	16	1.653
7	18	1.790
8	20	1.945
9	22	2.124
10	24	2.331
11	26	2.573
12	28	2.855
13	30	3.187
14	32	3.762
15	34	4.052
16	36	4.621
17	38	5.315
18	40	6.162

#### **2.4 Preparation of protein samples for steady-state and time-resolved fluorescence anisotropy measurements:**

Prior to every experiment the fluorescently labeled protein was concentrated using 3kDa molecular weight cut-off (MWCO) AMICON filter (purchased from Millipore) and passed through 50 kDa MWCO AMICON filter to remove higher order species formed if any. The concentration of protein was checked by measuring absorbance using UV-Vis spectrophotometer. The concentration of labeled protein was determined by using  $\epsilon_{340\text{ nm}} = 6,100\text{ M}^{-1}\text{ cm}^{-1}$ . For the preparation of samples, corresponding amount of sucrose (according to Table 1) was accurately weighed using a microbalance and labeled protein was added to maintain a final concentration of protein as 5  $\mu\text{M}$  for the final weight of the sample as 2 gm. The final weight of the sample was made up by adding native buffer (20 mM Tris, 50 mM NaCl, pH 7.4). The mixture was vortexed in order to dissolve sucrose and obtain a homogeneous solution. The solution was used for further experiments.

#### **2.5 Preparation of fluorescein samples for steady-state and time-resolved fluorescence anisotropy measurements:**

For the preparation of samples, corresponding amount of sucrose (according to Table 1) was accurately weighed using a microbalance and fluorescein was added to maintain a final concentration of 100 nM for the final weight of the sample as 2 gm. The weight of the sample was made up by adding native buffer (20 mM Tris, 50 mM NaCl, pH 7.4). The mixture was vortexed in order to dissolve sucrose and obtain a homogeneous solution. The solution was used for further experiments.

#### **2.6 Circular Dichroism (CD) experiments:**

The CD spectra were collected by fixing the concentration of labeled protein as 10  $\mu\text{M}$ . CD spectra were collected using Chirascan CD spectrometer (Applied Photophysics, UK) at 20°C using a quartz cuvette with path length 1 mm. The spectra were collected in the presence and absence of sucrose for all concentrations of sucrose with a scan rate of 1nm/s and averaged over 5 scans. The scan range was fixed for all samples as 200 nm-260 nm. All the spectra were buffer subtracted followed by smoothing using Chirascan 'ProData viewer' software provided along with the instrument.<sup>18</sup>

## 2.7 Steady-state fluorescence measurements:

All steady-state experiments were performed on Fluoromax-4 (Horiba Jobin Yvon, NJ) using 10 mm x 10 mm quartz cuvette at 20°C. For anisotropy measurements, the concentration of A18C  $\alpha$ -synuclein was fixed as 5  $\mu$ M and concentration of fluorescein was fixed as 100 nM. The steady-state anisotropy is given by the following equation

$$r = (I_{\parallel} - GI_{\perp}) / (I_{\parallel} + 2GI_{\perp})$$

where  $I_{\parallel}$  and  $I_{\perp}$  are fluorescence intensities collected using parallel and perpendicular geometries of the polarizers respectively. Respective G-factors (G) were used to correct the perpendicular components. For recording fluorescence anisotropy, excitation wavelength was fixed as 375 nm for IAEDANS labeled A18C  $\alpha$ -synuclein and at 485 nm for fluorescein and the excitation bandpass was fixed at 1 nm, whereas emission wavelength was fixed at the maxima of each sample with a bandpass of 4 nm. The integration time was 2 s.

## 2.8 Time-resolved fluorescence measurements:

The time-resolved fluorescence anisotropy decays were collected for all the samples using a time-correlated single photon counting (TCSPC) setup (Fluorocube, Horiba Jobin Yvon, NJ) at 20°C. 375 nm LASER was used as excitation source having a repetition rate of 1MHz for IAEDANS labeled protein samples and 485 nm LASER was used as excitation source having a repetition rate of 1 MHz for fluorescein samples. The parallel [ $I_{\parallel}(t)$ ] and perpendicular [ $I_{\perp}(t)$ ] intensity decays were collected by setting the emission monochromator at 0° and 90° orientation with respect to the excitation polarization. Bandpass was kept constant at 8nm for all measurements and a PhotoMultiplier Tube (PMT) (Hamamatsu Corp) was used as a detector. [ $I_{\parallel}(t)$ ] and [ $I_{\perp}(t)$ ] were globally analyzed and time-resolved anisotropy decay profiles were constructed using the following relationships:

$$I_{\parallel}(t) = I(t)[1 + 2r(t)]/3 \quad \dots\dots\dots(2)$$

$$I_{\perp}(t) = I(t)[1 - r(t)]/3 \quad \dots\dots\dots(3)$$

The anisotropy decay profiles delineated biexponential depolarization kinetics and two components  $\phi_{\text{fast}}$  and  $\phi_{\text{slow}}$  were recovered using the equation<sup>-11</sup>

$$r(t) = r_0 [\beta_{fast} \exp(-t/\phi_{fast}) + \beta_{slow} \exp(-t/\phi_{slow})] \dots\dots\dots (4)$$

Where  $r_0$  is the initial time-zero anisotropy,  $\phi_{fast}$  and  $\phi_{slow}$  are two rotational correlation time components with  $\beta_{fast}$  and  $\beta_{slow}$  being their corresponding amplitudes. The goodness of fit was assessed by reduced  $\chi^2$  values and randomness of residuals.<sup>11</sup>

A 2% solution of ludox in water was used to collect the instrument response function (IRF) ~265 ps. For obtaining a good signal-to-noise ratio, 10,000 counts were collected at the peak for IAEDANS and 20,000 counts were collected at the peak for fluorescein.

The time-resolved fluorescence data were analyzed by a decay analysis program that was provided by Prof. N. Periasamy (Retd. TIFR Mumbai)

### 3. Results and discussion

#### 3.1 Circular Dichroism (CD) measurements:

The study was initiated by selecting an appropriate viscosogen for preparing solutions of various viscosities. The presence of the selected viscosogen should not affect the native conformation of the protein monomer. We selected sucrose as the viscosogen for the study because the presence of sucrose did not alter the secondary structure of the protein, which was confirmed by the circular dichroism measurements. For sucrose concentrations ranging between 0% (w/w) to 40% (w/w), a characteristic random coil peak was observed around 200 nm confirming that the protein remained in random coil conformation for final sucrose concentration upto 40% (w/w). The measurements were done at experimental temperature, i.e. 20°C.

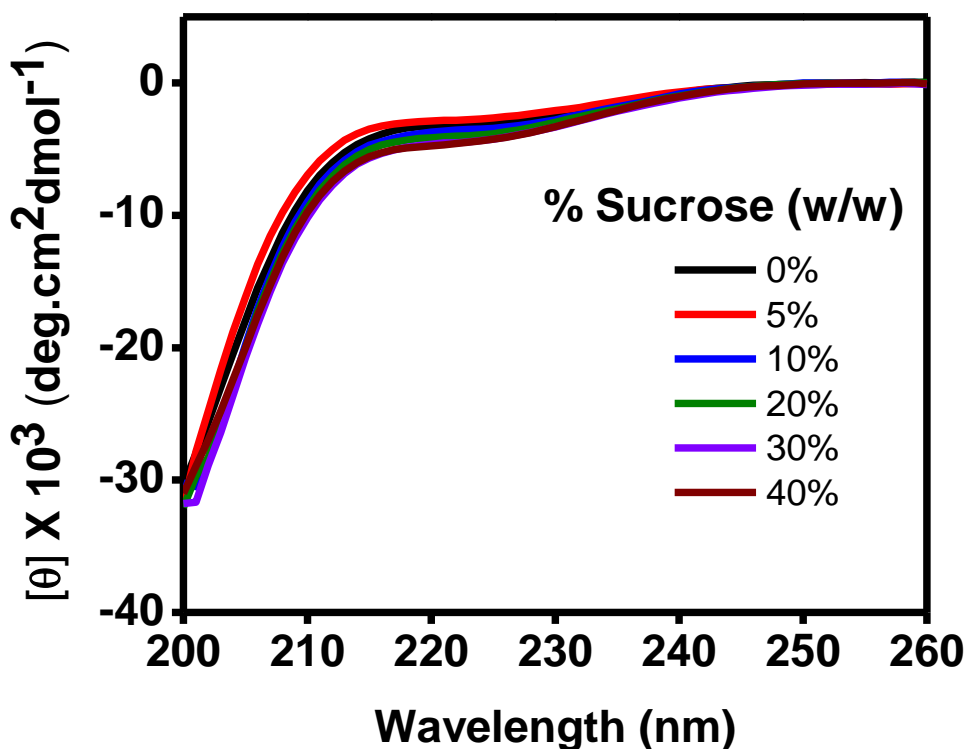


**Figure 4** CD spectra of IAEDANS-labeled A18C  $\alpha$ -synuclein in different concentrations of sucrose.

## 3.2 Steady-state fluorescence anisotropy measurements:

### 3.2.1 Rotational dynamics of free probe (fluorescein):

The rotational dynamics of a free particle in a solvent is described using the Stokes-Einstein-Debye (SED) theory. The theory relates the rotational correlation time ( $\phi$ ) of a particle to the temperature and viscosity of the solvent provided the rotational dynamics is described by a single rotational correlation time.<sup>19</sup> In order to confirm whether a free particle or a small molecule follows the SED model, we studied the rotational dynamics of free fluorescein in different concentrations of sucrose ranging from 0% (w/w) to 40% (w/w). In order to study the rotational dynamics of fluorescein we performed steady-state fluorescence anisotropy measurements. Fluorescence anisotropy provides information about the rotational mobility of a fluorophore (fluorescein in this case). Therefore, for slow molecular tumbling the anisotropy is high and vice versa. Increase in solvent viscosity will restrain the rotational mobility of the probe and hence we expected an increase in steady-state anisotropy with increase in the overall solvent viscosity. The SED equation is as follows:

$$\phi = \frac{\eta V}{k_B T} (fC) \quad \text{Where } \eta = \text{Dynamic viscosity of solvent, } \phi = \text{Rotational correlation time,}$$

$V$  = Molecular volume,  $f$  = Shape factor,  $C$  = Solute-solvent coupling parameter

$T$  = Temperature and,  $k_B$  = Boltzmann constant.<sup>8</sup>

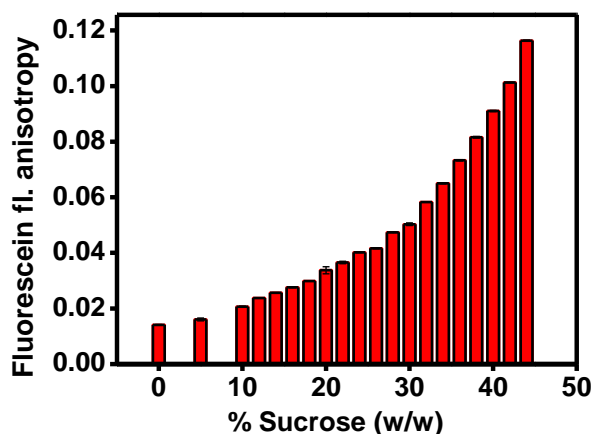


**Figure 5.** Steady increase observed in the steady-state anisotropy with increase in sucrose content.

The steady-state anisotropy was seen to increase steadily with an increase in the percentage of sucrose in the solution. The steady-state anisotropy value increased from 0.014 (for 0% sucrose) to 0.091 (for 40% sucrose). However, steady-state anisotropy depicts an average illustration of the concerned system and cannot be used to quantify the rotational dynamics of the fluorophore. Hence, we went on to perform highly sensitive picosecond time-resolved anisotropy measurements (discussed in detail in section 3.3).

### 3.2.2 Dynamics of IAEDANS-labeled human $\alpha$ -synuclein:

We then went on to see the effect of increasing solvent viscosity on the protein dynamics. We performed steady-state fluorescence anisotropy measurements and observed a steady increase in steady-state anisotropy of IAEDANS-labeled  $\alpha$ -synuclein. Figure 6 (b) shows cartoon representation of IAEDANS-labeled human  $\alpha$ -synuclein protein.

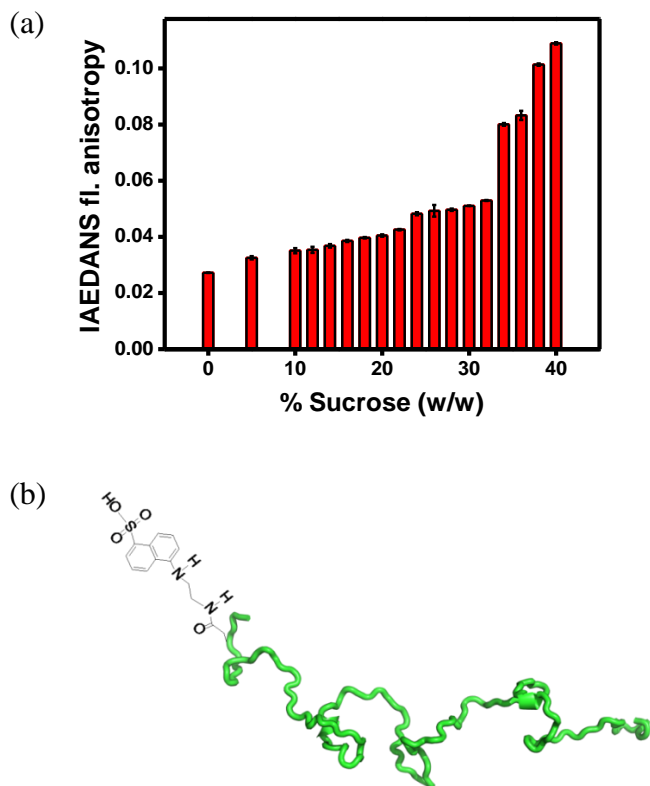


**Figure 6:** (a) Steady increase in IAEDANS anisotropy observed for IAEDANS-labeled  $\alpha$ -synuclein  
(b) Schematic representation of IAEDANS-labeled human  $\alpha$ -synuclein protein. (PcDB: 9AAC)

### 3.3 Time-resolved anisotropy measurements:

#### 3.3.1 Time-resolved anisotropy measurements of fluorescein:

We opted to use highly sensitive and powerful picosecond time-resolved anisotropy measurements in order to quantify the different modes of rotational relaxation of the protein backbone. The time-resolved fluorescence anisotropy decay measurements were performed using TCSPC setup. The fluorescence depolarization kinetics revealed a single exponential decay with an initial anisotropy of 0.4 to 0. Following table summarizes the recovered parameters. The rotational correlation time ( $\phi$ ) thus obtained was seen to increase with increase in solvent viscosity. An overlay of some of the representative decay profiles revealed that the rotational mobility of fluorescein was indeed getting dampened due to an increase in solvent viscosity as expected from the SED model. Rotational correlation time was observed to scale linearly with the solvent viscosity (refer table 1 for viscosity values). No intercept was obtained on the Y-axis (Figure 7 b) and hence the rotational dynamics of free probe, i.e. fluorescein was observed to follow the standard SED model at 20° C.

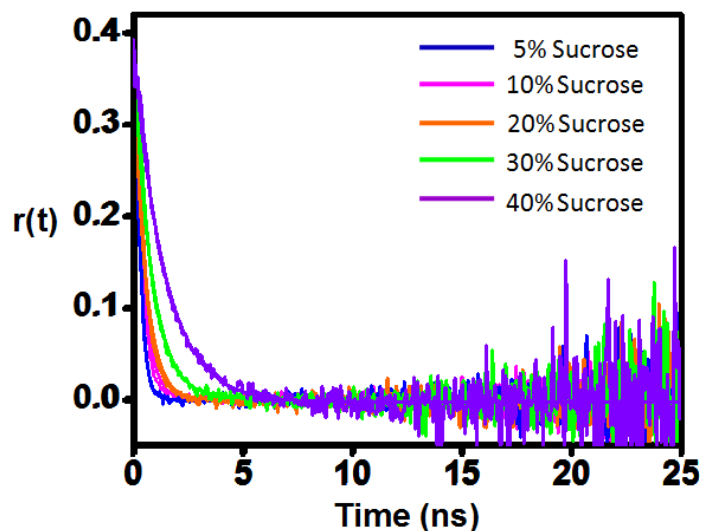


**Figure 7 (a):** Picosecond time-resolved anisotropy decays of fluorescein [ $r(t)$ ] in different solvent viscosities. (Data analysis was done by Ms. Debapriya Das)



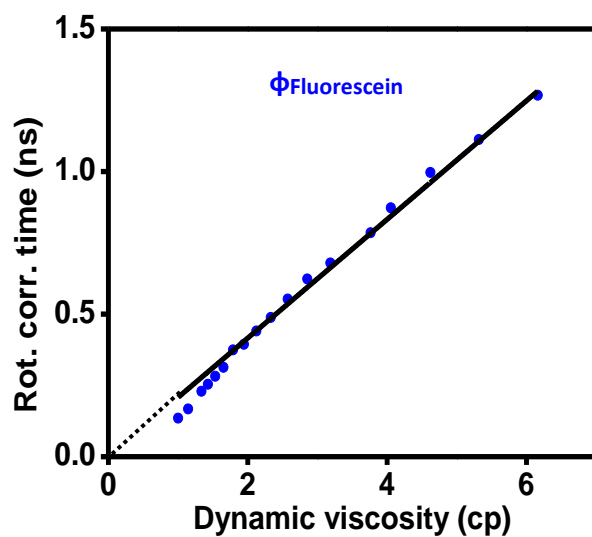


**Figure 7 (b):** Linear fit between rotational correlation time ( $\phi$ ) of fluorescein and the solvent viscosity (in centipoise)

**Table 2:** Rotational correlation time of fluorescein in different concentrations of sucrose.

Sucrose % (w/w)	$\phi$ (ns)	$\chi^2$
0	0.135	1.95
5	0.167	1.43
10	0.229	1.67
12	0.254	1.76
14	0.282	1.64
16	0.313	1.58
18	0.374	1.44
20	0.394	1.65
22	0.441	1.52
24	0.488	1.48
26	0.553	1.40
28	0.623	1.51
30	0.679	1.58
32	0.780	1.41
34	0.873	1.42
36	0.997	1.30
38	1.112	1.45
40	1.267	1.43

### 3.3.2 Time-resolved fluorescence anisotropy measurements for protein

In order to distinguish between different rotational relaxation modes arising from different dynamical events we took advantage of picosecond time-resolved fluorescence anisotropy measurements. The fluorescence depolarization kinetics of a fluorophore-tagged globular collapsed protein delineates biexponential decay profile consisting of a fast rotational correlation time ( $\phi_{\text{fast}}$ ) which arises due to the local diffusional motion of the fluorophore and a slow rotational correlation time ( $\phi_{\text{slow}}$ ) which arises due to global tumbling of the protein and is related to the hydrodynamic radius of the protein.<sup>22</sup>

Our previous studies revealed that in case of expanded IDPs, such as  $\alpha$ -synuclein, the second or slow rotational correlation time ( $\phi_{\text{slow}}$ ) arises due to collective segmental torsional mobility of the polypeptide backbone.<sup>11</sup> The origin of this torsional mobility lies in the Ramachandran  $\Phi$ - $\Psi$  dihedral angle rotations in the protein backbone.<sup>21</sup> (Figure 9).

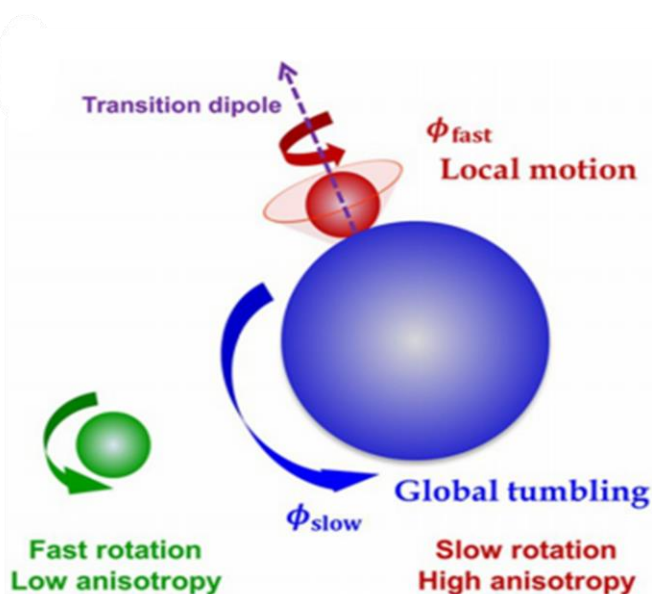


Image courtesy: Majumdar A., Mukhopadhyay S., (2018), *Methods Enzymol*

**Figure 8:** Different modes of fluorescence depolarization arising due to different dynamical events. (Reused with permission from [21])

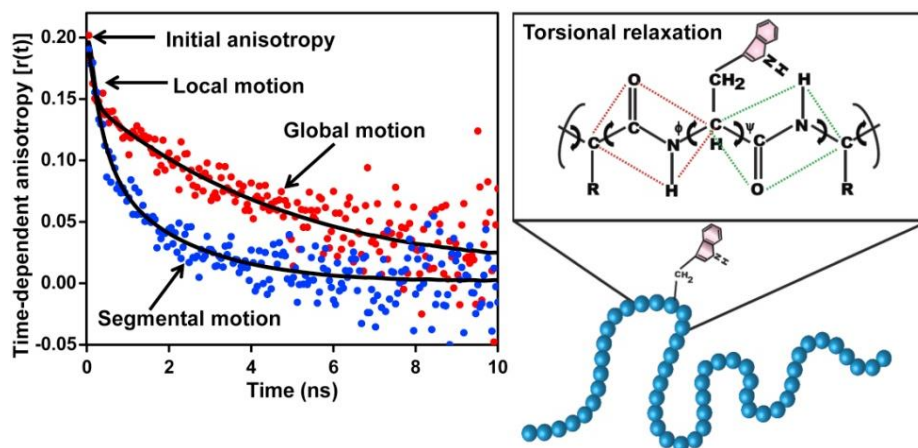
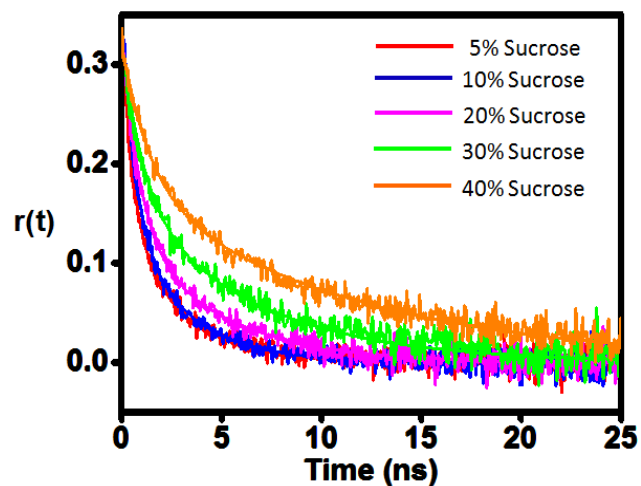


Image courtesy: Mukhopadhyay and coworkers (2016) *Biophysical Journal*

**Figure 9:** Fluorescence anisotropy decay profiles obtained in case of globular/collapsed proteins vs. IDPs. The segmental mobility arises due to the backbone torsional relaxation in the  $\Phi$ - $\Psi$  dihedral space (Reproduced with permission from [11])

Our studies showed that fluorescence depolarization kinetics of IAEDANS-labeled  $\alpha$ -synuclein revealed biexponential decay from an initial anisotropy of 0.3 to 0 and two distinct rotational correlation time components were obtained for all concentrations of sucrose. An overlay of some of the representative decay profiles (Figure 10) revealed that the fast as well as slow rotational correlation time component was changing with a change in the solvent viscosity value. In order to understand the data better, we plotted  $\phi_{\text{fast}}$  and  $\phi_{\text{slow}}$  as a function of solvent viscosity. (Figure 10 b).  $\phi_{\text{slow}}$  was observed to increase with an increase in the solvent viscosity (Refer table 2). We observed that the fast rotational correlation time component increased with increase in solvent viscosity however it did not scale linearly with the solvent viscosity. On the contrary, the slow rotational correlation time component yielded an intercept ( $\sim 1.04$  ns) on the Y-axis. We would further perform rigorous analysis and experiments for understanding the behavior of  $\phi_{\text{fast}}$  as a function of solvent viscosity since we expect the fast rotational correlation time component to follow the traditional SED model and scale linearly with solvent viscosity.



**Figure 10(a):** Picosecond time-resolved anisotropy decays of IAEDANS-labeled  $\alpha$ -synuclein [ $r(t)$ ] in different solvent viscosities. (Data analysis was done by Ms. Debapriya Das)

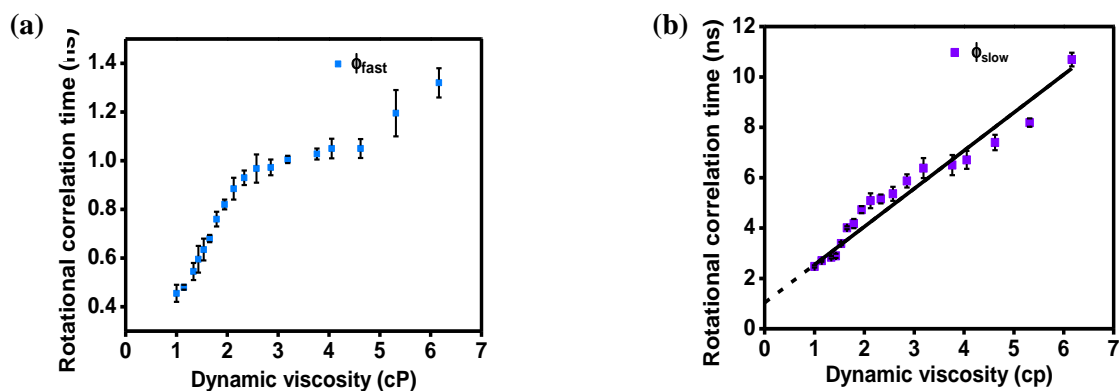


**Figure 10:** (a)  $\phi_{\text{slow}}$  plotted as a function of solvent viscosity (b) Linear fit between the slow rotational correlation time components and dynamic viscosity of the solvent.

**Table 3:** Rotational correlation time components and their corresponding amplitudes for IAEDANS-labeled A18C  $\alpha$ -synuclein.

Sucrose % (w/w)	$\phi_{\text{fast}}$ (ns)	$\phi_{\text{slow}}$ (ns)	$\chi^2$	$\beta_{\text{fast}}$	$\beta_{\text{slow}}$
0	0.455±0.035	2.475±0.045	1.665±0.015	0.615±0.01	0.385±0.03
5	0.48±0.01	2.70±0.04	1.68±0.03	0.575±0.00	0.425±0.00
10	0.545±0.035	2.84±0.05	1.65±0.01	0.555±0.00	0.445±0.005
12	0.595±0.055	2.895±0.085	1.645±0.045	0.535±0.02	0.465±0.02
14	0.635±0.045	3.38±0.06	1.855±0.035	0.465±0.02	0.43±0.01
16	0.68±0.03	4.01±0.06	1.915±0.025	0.565±0.01	0.435±0.01
18	0.76±0.03	4.175±0.185	1.845±0.025	0.595±0.005	0.405±0.00
20	0.82±0.02	4.73±0.14	1.73±0.03	0.57±0.01	0.43±0.01
22	0.885±0.045	5.085±0.295	1.825±0.045	0.60±0.01	0.40±0.01
24	0.93±0.03	5.1525±0.17	1.735±0.065	0.56±0.01	0.44±0.01
26	0.968±0.058	5.359±0.281	1.705±0.105	0.6±0.01	0.40±0.01
28	0.9725±0.0325	5.87±0.26	1.50±0.02	0.53±0.02	0.47±0.02
30	1.005±0.015	6.38±0.4	1.68±0.04	0.455±0.03	0.545±0.03
32	1.0275±0.0225	6.50±0.4	1.71±0.04	0.46±0.02	0.54±0.02
34	1.05±0.04	6.705±0.355	1.805±0.035	0.48±0.01	0.52±0.01
36	1.057±0.039	7.395±0.305	1.8±0.03	0.48±0.01	0.52±0.01
38	1.195±0.095	8.185±0.165	1.76±0.06	0.435±0.02	0.565±0.02
40	1.32±0.06	10.645±0.255	1.855±0.035	0.455±0.00	0.545±0.005

To visualize the entire data we constructed a scatter plot of the rotational time components for fluorescein and IAEDANS-labeled protein as a function of solvent viscosity. The scatter plot of  $\phi_{\text{fluorescein}}$ ,  $\phi_{\text{fast}}$  and  $\phi_{\text{slow}}$  of IAEDANS-labeled protein as a function of solvent viscosity showed that the fast rotational time component for the fluorophore tagged protein scaled up with the rotational correlation time of the free probe, i.e. fluorescein (Figure 11). Therefore the local diffusional motion of the dye is similar to that of a free particle in the dense aqueous environment and follows the standard SED model of hydrodynamics. On the contrary, the slow rotational correlation time component was seen to behave distinctly different from the fast component and did not scale according to the SED model. These results indicate that the

local motion fluorophore is affected due to the solvent viscosity alone. This component therefore changes due to the wet friction experienced by the fluorophore.

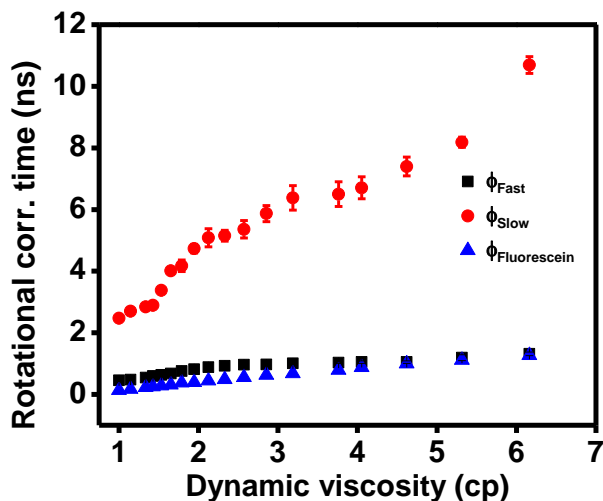


**Figure 11:** Scatter plot showing the fast rotational correlation time component scaling up with the rotational correlation time of fluorescein.

In order to get a better understanding of the data we constructed a normalized plot between  $\phi$  and solvent viscosity (Figure 12).

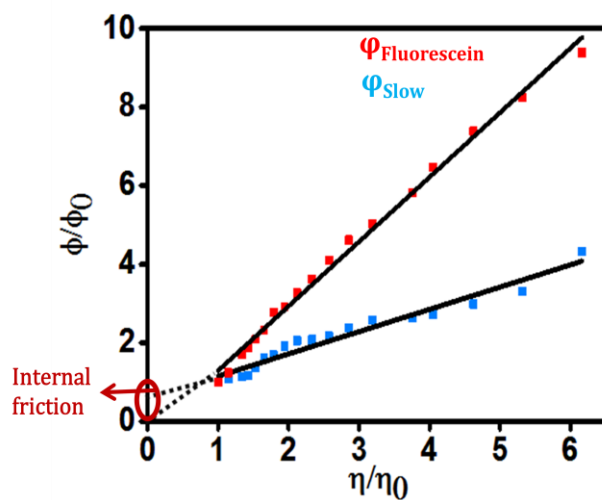


**Figure 12:** Normalized plot reveals that the rotational correlation time of fluorescein scales linearly with solvent viscosity and does not give rise to an intercept on the Y-axis, unlike the slow rotational correlation time component of IAEDANS-labeled protein.

#### 4. Conclusion and future outlook

Studying protein dynamics in case of disordered proteins is of great concern. The conformational plasticity displayed by IDPs could be attributed to the low internal friction experienced by these proteins as it has been previously reported that the sequence composition of a protein plays a significant role in determining the internal friction experienced by the protein.<sup>22, 23</sup> Therefore elucidating the molecular origin of internal friction in case of IDPs will help us understand some of the astonishing properties displayed by these proteins.<sup>24</sup>

From our picosecond time-resolved fluorescence anisotropy readouts we confirmed that the rotational dynamics of a free probe, fluorescein, follows the standard Stokes-Einstein-Debye model as the rotational dynamics is controlled solely by the “wet friction” arising due to solvent viscosity. However, even at zero solvent viscosity the protein is seen to offer some resistance towards changing its conformation since the slow rotational correlation time component yields an intercept on the Y-axis when plotted against solvent viscosity. We suspect that this internal resistance offered by the protein arises due to the collective segmental torsional mobility of the polypeptide backbone which indeed arises as the protein explores the Ramachandran  $\Phi$ - $\Psi$  dihedral space. We speculate that the “roughness” of the energy landscape, in case of human  $\alpha$ -synuclein, is a result of the underlying local barrier crossing events, in particular the dihedral rotations. These barrier crossing events are thus insensitive to the solvent viscosity and give rise to internal friction or the “dry” friction experienced by the protein. Our studies can thus provide an insight into the molecular origin of internal friction in case of human  $\alpha$ -synuclein, an extended IDP, and can be further used for understanding the dynamics of other expanded intrinsically disordered proteins.

Future studies will help us quantify internal friction arising due to dihedral relaxation in case of IDPs. Since the internal friction arising due to dihedral isomerization is independent of the nature of the amino acid side chain, we will carry out similar experiments for other residue positions. We also aim at verifying the deviation of the conformational relaxation time from its first power law dependence on solvent viscosity.

## 5. Bibliography

1. Uversky Vladimir (2003) A Protein-Chameleon: Conformational Plasticity of  $\alpha$ -Synuclein, a Disordered Protein Involved in Neurodegenerative Disorders. *J. Biomol. Struct. Dyn.* 21:211-34.
2. Kramers HA (1940) Brownian motion in a field of force and the diffusion model of chemical reactions. *Physica* 7:284-304
3. Soranno Andrea, Stucki-Buchli Brigitte, Nettels Daniel, Cheng Ryan, Mueller-Spaeth Sonja, Pfeil Shawn, Hoffmann Armin, A. Lipman Everett, E. Makarov Dmitrii and, Schuler Benjamin (2012) Quantifying internal friction in unfolded and intrinsically disordered proteins with single-molecule spectroscopy. *PNAS.* 109:17800–17806
4. Echeverria Ignacia, E Makarov Dmitrii, Papoian Garegin (2014) Concerted Dihedral Rotations Give Rise to Internal Friction in Unfolded Proteins. *Journal of the American Chemical Society.* 136:8708-8713
5. Kubela J, Hofrichter J, Eaton WA (2004) The protein folding ‘speed limit’. *Curr Opin Struct Biol* 14:76-88
6. Borgi Alessandro, Wensley BG, Soranno Andrea, Nettels Danielv, Borgia MB, Hoffmann Armin, Pfeil SH, Lipman EA, Clarke Jane and, Schuler Benjamin (2012) Localizing internal friction along the reaction coordinate of protein folding by combining ensemble and single-molecule fluorescence spectroscopy 3:1195
7. Best RB, Hummer G (2011) Diffusion models of protein folding. *Phys Chem Chem Phys* 13:16902-16911
8. Dutt GB, Doraiswamy S, Periasamy N (1990) Rotational reorientation dynamics of polar dye molecular probes by picosecond laser spectroscopy. *J Chem Phys.* 93:8498-8513
9. Hagen SJ, Linlin Qiu, Suzette Pabit (2005) Diffusional limits to the speed of protein folding: Fact or friction? *J. Phys: Condens. Matter.* 17: 1503-1514
10. Hagen SJ (2011) Solvent viscosity and friction in protein folding dynamics. *Curr Protein Pept Sci.* 11:385-395



11. Jain N, Narang D, Bhasne K, Arya S, Bhattacharya M and, Mukhopadhyay S (2016) Direct observation of the intrinsic backbone torsional mobility of disordered proteins. *Biophys J.* 111:768-774
12. Anfinsen CB, Haber E, Sela M, White FN (1961) The kinetics of formation of native ribonucleases during oxidation of the reduced polypeptide chain. *PNAS* 47:1309-1314
13. Dunker AK et. al. (2001) Intrinsically disordered protein. *J Mol Graph Model* 19:26-59
14. Weinreb PH, Zhen W, Poon AW, Conway KA, Lansbury PT, Jr, (1996) NACP, a protein implicated in Alzheimer's disease and learning, is natively unfolded. *Biochemistry* 35:13709-13715
15. Tamamizu-Kato S, et al. (2006) Calcium-triggered membrane interaction of  $\alpha$ -synuclein acidic tail. *Biochemistry* 45:10947-10956
16. Van Raaij ME, Ine MJ, Segers-Nolten, I.M.J.; Subramaniam V (2006) Quantitative morphological analysis reveals ultrastructural diversity of amyloid fibrils from  $\alpha$ -synuclein mutants. *Biophys. J.* L96-98
17. Haynes William M, *CRC Handbook of chemistry and physics.* (97<sup>th</sup> edition 2016-2017), CRC press, ISBN 10- 9781498754293
18. MS Thesis (2013) Karishma Bhasne
19. Das A, Biswas R, Charabarti J (2012) Solute rotation in polar liquids: Microscopic basis for the Stokes-Einstein-Debye model. *J. Chem. Phys.* 136:014505-1-014505-8
20. Jain N, Bhattacharya M, Mukhopadhyay S (2011) Chain Collapse of an Amyloidogenic Intrinsically Disordered Protein. *Biophys. J.* 101: 1720-1729
21. Majumdar A, Mukhopadhyay S (2018) Fluorescence Depolarization Kinetics to Study the Conformational Preference, Structural Plasticity, Binding, and Assembly of Intrinsically Disordered Proteins. *Methods Enzymol.* 611, 347-382
22. Cheng RR, Hawk AT, Markov DE (2013) Exploring the role of internal friction in the dynamics of unfolded proteins using simple polymer models. *J. Chem. Phys.* 138:074112

23. Moglich A, Joder K, Kiefhaber T (2006) Excluded volume, local structural cooperativity, and the polymer physics of protein folding rates. PNAS 104:10841-10846
24. Dunker AK, Silman I, Uversky VN, Sussman JL (2008) Function and structure of inherently disordered proteins. Curr. Opin. Struct. Biol. 18:756-764
25. Moglich A, Joder K, Kiefhaber T (2006) End-to-end distance distributions and intrachain diffusion constants in unfolded polypeptide chains indicate intramolecular hydrogen bond formation. PNAS 103:12394-12399
26. Schuler B, Lipman EA, Eaton WA (2002) Probing free-energy surface for protein folding with single-molecule fluorescence spectroscopy. Nature 419:743-747
27. Zheng W, Hofmann H, Schuler B, Best RB (2018) Origin of internal friction in disordered proteins depends on solvent quality. J. Phys. Chem. B. 122:11478-11487
28. Jain N, Bhasne K, Hemaswathi M, Mukhopadhyay S (2013) Structural and Dynamical Insights into the Membrane-Bound  $\alpha$ -Synuclein, PLoS ONE 8(12): e83752
29. Lee R et. al., (2014) Classification of intrinsically disordered regions and proteins. Chem. Rev. 114:6589-66331